Preparation and flame retardancy of 3-(hydroxyphenylphosphinyl)-propanoic acid esters of cellulose and their fibers

Yunbo Zheng · Jun Song · Bowen Cheng · Xiaolin Fang · Ya Yuan

Abstract New 3-(hydroxyphenylphosphinyl)-propanoic acid (3-HPP) esters of cellulose were synthesized in N, N-dimethylacetamide/LiCl homogeneously by the method of in situ activation with p-toluenesulfonyl chloride. Chemical structure and thermal properties of the cellulose esters were investigated by FTIR, ^{13}C-NMR, TGA, RT-IR and Py–GC/MS, and their flame retardancy was studied by limiting oxygen index (LOI) test and vertical flammability test. It was found that the degree of substitution (DS) of cellulose esters, in the range from 0.62 to 1.42, had an obvious effect on solubility of cellulose esters. According to the FT-IR and Py–GC/MS results, flame retardant 3-HPP reacting with cellulose could accelerate dehydration action and decrease flammable released products. Besides, ESEM observation also confirmed that flame retardant cellulose (FRC) fibers with 3 wt% cellulose acetate prepared by dry-wet spinning technique possessed good flame resistance.

Keywords Cellulose · Homogeneous modification · Fire-retardant fiber

Y. Zheng · J. Song · B. Cheng · X. Fang · Y. Yuan
Key Laboratory of Tianjin City Modification and Functional Fiber, Department of Materials Science and Engineering, Tianjin Polytechnic University, Tianjin 300387, China
e-mail: bowen15@tjpu.edu.cn

J. Song (✉) · B. Cheng
State Key Laboratory of Hollow Fiber Membrane Materials and Processes, Department of Materials Science and Engineering, Tianjin Polytechnic University, Tianjin 300387, China
e-mail: sjhb2000@163.com

Introduction

Cellulose is an abundant and renewable resource, and garments made from it are usually comfortable and breathable. As a result, cellulose fiber has become one of the most commonly employed textile fibers. However, cellulose generally is readily flammable [with limiting oxygen index (LOI) of 18.4 %], which has restricted its wide application (Lewin 2010). Therefore, much effort has been made for imparting flame retardancy of cellulose fiber by halogen-free flame retardant in an economically and environmentally friendly manner.

In the past few years, there have been many successes in improving flame retardancy of textile (Hong et al. 2009; Horrocks 2011; Liang et al. 2013). Several strategies, including pad-dry-cure, graft polymerization, multistep sol–gel and layer-by-layer assembly, have been used to confer flame retardancy properties of cotton cellulose (Alongi et al. 2014b). Thach-Mien Nguyen et al. prepared the flame

retardant cotton cellulose by pad-dry-cure to study the structural effect of phosphoramidate derivatives (Alongi et al. 2014b). Reddy et al. (2005) modified flame retardant cotton fabric by ionizing radiation graft polymerized method. Jenny Alongi and co-workers treated cotton fabrics by sol–gel processes in order to create a silica compact coating on the fibers to enhance their thermal stability and flame retardancy (Reddy et al. 2005). Chang et al. (2014) applied successfully flame-retardant nanocoatings to cotton fabrics by a continuous layer-by-layer deposition process. Some inventions also produce cellulose fibers with fire retardance. Rüf et al. (2010) patented the preparation of flame retardant Lyocell fibers by adding inorganic additives during the spinning process. Bell et al. (1997) provided a method of forming flame retardant cellulose fibers by incorporating a flame retardant chemical into the fibers whilst the fiber is in the never-dried condition prior to first drying. Nevertheless, the above mentioned techniques often require complicated conditions and complex procedures, which have deleterious effects on the mechanical properties of the treated cotton fabrics (Huang et al. 2012). In addition, moisture regain and poor resistance to washing usually lead to an imperfect modification of flame retardant cotton fabric (Alongi et al. 2014b; Siriviriyanun et al. 2008).

Homogeneous chemical modification is the most important tool to obtain cellulose with functional groups (Gräbner et al. 2002; Liebert and Heinze 2005; Tsvetkov et al. 2013). Among all solvents of cellulose, DMAc/LiCl is a non-derivatizing and non-aqueous solvent system, and has been widely employed for analysis of cellulose and for preparation of a wide variety of derivatives without significant degradation under homogenous reaction conditions (Liebert 2010; Raus et al. 2012; Strlič and Kolar 2003). By contrast, esterification of cellulose with carboxylic acids through in situ activation by sulfonic acid chlorides is a relatively new modification route, in which the introduction of a wide range of carboxyl-functionalized substituents can be controlled effectively (Hasani and Westman 2007).

Up to now, various kinds of flame retardants, such as halogen derivatives (Schnipper et al. 1995), inorganic additive (Horrocks et al. 2005), boron-containing (Martin et al. 2006), nitrogen based (Lu and Hamerton 2002) and organic phosphorus compounds (Yang and Yang 2008; Yuan et al. 2012b), have been introduced to natural cellulose. Unlike these flame retardants, halogen-free phosphorus compounds are likely to be the promising flame retardant candidates for cotton cellulose, since these environmentally friendly compounds can catalyze the dehydration of cellulose as the char former under acid condition, thus reducing the formation of flammable volatiles and smoke (Rupper et al. 2010; Yoshioka-Tarver et al. 2012).

In our previous research, interest has mainly focused on modification and processing of cellulose (Lu et al. 2012; Lu et al. 2014). In this paper, 3-(hydroxyphenylphosphinyl)-propanoic acid esters of cellulose were prepared using in suit activation with Tos-Cl in DMAc/LiCl, and then the thermal property and flame retardancy of the cellulose esters were studied. Afterwards, the cellulose esters were dissolved in conventional organic solvents to spin flame retardant fibers, and the mechanical property and flame resistance of the fibers were discussed.

Experimental

Materials

Cellulose (DP = 630), supplied by Jilin Chemical fiber CO. LTD., China, was treated in a vacuum oven at 95 °C for 12 h to remove any moisture before use. DMAc, anhydrous LiCl and Tos-Cl were purchased from Kermel Chemical CO. LTD., China. 3-HPP was acquired from kaixin Chemical CO. LTD., China. DMAc was dried and distilled before use according to conventional methods. Anhydrous LiCl was dried at 130 °C for 10 h under vacuum. Other reagent grade chemicals were used without further purification.

Methods

Dissolution of cellulose in DMAc/LiCl

For a typical preparation, 1.0 g (6.2 mmol) dried cellulose and 40 mL DMAc were kept at 130 °C for 2 h under stirring in a dry nitrogen atmosphere to obtain a slurry. After the slurry temperature dropped to 100 °C, 3 g anhydrous LiCl was added. Then, the mixture was cooled down to room temperature under stirring, and the cellulose could be dissolved completely within some hours.

Esterification reaction of cellulose with 3-HPP/Tos-Cl

3.96 g 3-HPP (18.6 mmol) and 3.53 g (18.6 mmol) Tos-Cl were dissolved in two copies of 10 mL DMAc, respectively. Then, the obtained two solutions were added to the cellulose solution containing 1 g (6.2 mmol) cellulose. After homogeneous reaction at 40 °C for 24 h, the product was precipitated in 300 mL ice water, filtered off, washed with water and ethanol, and dried in vacuum at room temperature.

Propionylation or acetylation of 3-HPP ester of cellulose (FRC)

Propionylated or acetylated of FRCs according to literatures (Hasani and Westman 2007; Köhler and Heinze 2007), in which 8 mL pyridine were carefully added into a solution of 0.2 g 3#FRC in 13 g 1-allyl-3-methylimidazolium chloride (AmimCl) kept at 40 °C. However, the reaction system turned into gelation (cross-linked) right away when propionic anhydride were dropwise added to the solution, which made mechanical stirring extremely difficult. The detailed explanation can be seen in Supporting Information.

Preparation of 3-HPP ester of cellulose (FRC) fibers

A certain amount of FRC (17 wt %) and cellulose acetate (3 wt%) were added into dimethyl sulfoxide (DMSO) to form 20 wt% homogeneous spinning solution at 80 °C under mechanical stirring. After degassing and filtering, the solution was extruded under a pressure of 0.2 MPa by dry–wet spinning procedure, and the process could last until the solution was exhausted. Here, the coagulation was distilled water, the spinning speed was 1.5 m/min, and the extruded speed for the solution was 2 mL/min.

Measurements

Fourier transform infrared spectroscopy (FT-IR) was performed on a Bruker TENSOR37 instrument with the KBr-technique. KBr tablets were dried at 100 °C for 1 h to remove moisture before the measurement. All spectra were recorded with an accumulation of 32 scans with a resolution of 4 cm^{-1} in the range of 4,000–500 cm^{-1}.

^{13}C NMR spectra were acquired on a Bruker AMX 400 MHz spectrometer. The cellulose ester was measured in DMSO-d$_6$ (100 mg/mL) at room temperature. The number of scans was in the range from 10,000 to 30,000.The content of phosphorus (%P) in the FRC was determined by ICP-9000(N + M) to calculate the degree of substitution (DS) according to the following equation:

$$DS = \frac{M_{AGU} * P\%}{M_P - M_{3-HPP} * P\% + M_{H_2O} * P\%},$$

where M_{AGU}, M_P, M_{3-HPP} and M_{H2O} denote the molar masses of the anhydroglucose unit, the phosphorus, the 3-HPP and the H$_2$O, respectively.

The LOI was measured according to GB/T2403-1993 by using JF-3 LOI instrument. The LOI tests were conducted on FRC membrane (13 cm × 6 cm). The vertical flammability was measured according to GB/T 5455-1997 by using CZF-3 instrument. The vertical flame tests were performed on FRC membrane (30 cm × 7.6 cm). The average values of 4–6 repetitive measurements were reported. The flame spread rate was calculated as follows: Rate of flame spread (mm/s) = char length (mm)/[x + after flame time (s)] (Muralidhara and Sreenivasan 2010), where x is application duration (12 s).

The thermogravimetric analysis (TGA) was carried out on the TGA Q5000 IR thermogravimetric analyzer (TA Instruments) using a heating rate of 10 °C/min from 20 to 600 °C under nitrogen atmosphere.

The thermo-oxidative degradation of the FRC was studied by real time Fourier transform infrared (RT-IR) method using Nicolet MAGNA-IR 750 spectrophotometer. Powders of the cured samples were mixed with KBr powders, and then the mixture was pressed into a tablet. Afterwards, the tablet was placed into the oven, and the temperature was raised at a heating rate of about 10 °C/min.

Pyrolysis–gas chromatography/mass spectrometry (Py–GC/MS) analysis was carried out on a system combined with a gas chromatography/mass spectrometry (6890GC/5973MSD, Agilent) and a Frontier Py-2020-type pyrolyzer. An AgilentHP-5 capillary column in size of 30 m × 0.25 mm × 0.25 μm was used. Testing conditions were as follows: carrier gas speed: 1.5 mL (He)/min; injector temperature: 250 °C, pyrolysis temperature: 600 °C, mass scanning range: 40–550 m/z, ionic detector: 250 °C. The

Scheme 1 Esterification of cellulose with 3-HPP
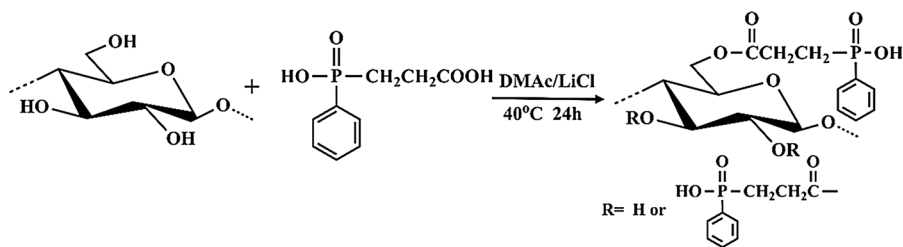
Table 1 Conditions for and results of the preparation of FRCs with 3-HPP in DMAc/LiCl

No.	Molar ratio[a]	DS[b]	Partial DS at position			Solubility[c]		
			6	3	2	DMSO	DMAc	THF
1#FRC	1:1:1	0.62	0.25	0.20	0.17	⊕	−	−
2#FRC	2:2:2	0.67	0.27	0.22	0.18	+	⊕	−
3#FRC	3:3:3	0.96	0.39	0.30	0.27	+	⊕	−
4#FRC	4:4:4	1.33	0.53	0.44	0.36	+	⊕	−
5#FRC	5:5:5	1.42	0.54	0.48	0.40	+	⊕	−

[a] Mole AGU/mole 3-HPP/mole Tos-Cl

[b] Degree of substitution

[c] Soluble (+), swelling (⊕), insoluble (−)

column was kept at 50 °C for 5 min, and then heated up to 230 °C at a rate of 10 °C/min. Afterwards, the column was maintained at 230 °C for 5 min.

Scanning electron microscopy (SEM; Japan Hitach S-4800) was used to study the morphological features of residual char of cellulose and FRCs. Environmental scanning electron microscope (ESEM; CzechQuan ta200) was used to observe the morphology of FRC fibers.

Tensile strength of the fibers was performed on XQ-1fiber tensile tester (LaiZhou Electron Instrument Co. Ltd., Shandong, China) with an extension speed of 10 mm/min under equilibrium conditions at 25 °C and 65 % relative humidity.

Results and discussion

Synthesis and characterization of FRCs

Scheme 1 shows the esterification of cellulose with 3-HPP at 40 °C for 24 h. From Table 1, it is noted that the DS of all FRCs increases with the ratio of AGU/3-HPP/Tos-Cl increasing and that the highest DS is 1.42 when the molar ratio reaches 1:5:5. Notably, different

distribution of the functional groups may lead to different solubility. The products obtained with cellulose are well soluble in DMSO when DS ≥ 0.67, so that DMSO is an important solvent for cellulose esters from a technical point of view, especially for fiber spinning.

FTIR spectra (Fig. 1) of FRCs present the typical absorptions of the cellulose backbone as well as signals of aromatics at 1,600, 1,530 and 1,421 cm^{-1}. Furthermore, the band at 1,731 cm^{-1} confirms the presence of the ester carbonyl group (C=O). It is obvious that the intensity of the C=O stretching band (1,731 cm^{-1}) increases with the increase of substitution degree (Sui et al. 2008).

Figure 2 shows the structure of the cellulose esters analyzed by ^{13}C-NMR spectroscopy in DMSO-d$_6$. Besides the carbon signals of modified AGU in the region of δ = 59.1–104.8 ppm, the resonances assigned to the carbon atoms of the 3-HPP moieties are visible at δ = 126–136 ppm (C-10–C-15), 24–26 ppm (C-9) and 26–28 ppm (C-8). Furthermore, the signal at 173–174.2 ppm which originates from the carbonyl carbon of the ester (C-7) linkage confirms the formation of ester. In addition, the signal at δ = 98.8 ppm can be assigned to C-1′ (C-1 atom
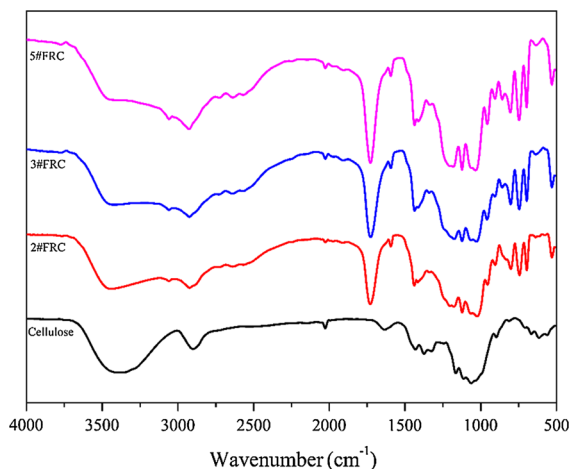
Fig. 1 FTIR spectra of cellulose and FRCs

influenced by O-2) (Hussain et al. 2004). Unfortunately, the spectrum is lack of resolution for exactly assigning signals of the carbons influenced by the esterification at C-2 and C-6 (C-2 and C-6 s respectively).

The partial DS values at C-6, C-3 and C-2 positions of FRCs were calculated from the integration of the carbonyl carbon area of the ^{13}C NMR spectroscopy (Cao et al. 2011; Wu et al. 2004), and the signal at 173.90 ppm was attributed to the carbonyl carbon at C-6 (C_6-7), 173.68 ppm to that at C-3 (C_3-7), and 173.37 ppm to that at C-2 (C_2-7). It can be exhibited different reaction activities of the three hydroxyl groups on cellulose backbone in Table 1. For instance, the 3#FRC with a total DS of 0.96 showed a partial DS at C-6 of 0.39, at C-3 of 0.30, at C-2 of 0.27. Obviously, the order of reactivity of the esterification of cellulose with 3-HPP is C-6 (–OH) > C-3 (–OH) > C-2 (–OH).

Flame retardant properties of the FRCs

Vertical flammability and LOI were employed to evaluate flame retardant properties of the FRCs (Table 2). The results show that esterification reaction with 3-HPP can decrease the flammability of cellulose. On the one hand, char length, afterflame and afterglow time are all changed significantly, so that the flame spread rate of the FRCs is also much lower than that of cellulose. On the other hand, with the increase of DS,

the LOI values of the FRCs are improved gradually and the highest LOI value can reach 38.7, which confirms that phosphorus-based compounds can enhance flame retardancy of cellulose effectively (Liu et al. 2012).

Thermal behavior

TGA curves of the FRCs and cellulose are presented in Fig. 3. Thermal degradation of cellulose can be divided into three stages: the initial stage around 100–120 °C, the second stage from 320 to 375 °C, and the final stage above 400 °C. In the initial stage, physical absorbed water is released and some physical properties of cellulose are damaged, with only a little weight loss (Shahidi 2014). The second stage is the main pyrolysis stage of cellulose, in which dehydration and decarboxylation reactions take place and combustible gases are produced in the crystalline region of cellulose (Shahidi 2014). Finally, when the temperature is above 400 °C, the residual char formed in the second stage is decomposed (Shafizadeh and Fu 1973; Wang et al. 2006).

It is known that the part of phosphorus-based flame retardant can lower the temperature for treating cellulose by 50–150 °C in the second stage (Nguyen et al. 2013). A similar phenomenon can be observed in Fig. 3. For all FRCs, release of water leads to a small weight loss in the first stage (210–230 °C), which can be attributed to the thermal decomposition or volatilization of flame retardant after dehydration. In the next stage (260–315 °C), the weight loss becomes more significant due to the evolution of most volatiles from the depolymerization of cellulose. Another important difference of cellulose and FRCs in TGA is the final char residue. It can be seen that the FRCs have more char residue than cellulose at 600 °C, which suggests that 3-HPP can change the pyrolysis mode of cellulose (Shahidi and Ghoranneviss 2014).

RT-IR analysis

RT-IR was used to evaluate thermal oxidative degradation of cellulose and the FRCs. Figure 4 shows the FTIR spectra of cellulose at different degradation temperatures. Neat cellulose presents characteristic absorption peaks at 3,400 cm^{-1} (O–H stretching), 2,910 cm^{-1} (C–H stretching), 1,650 cm^{-1} (absorbed
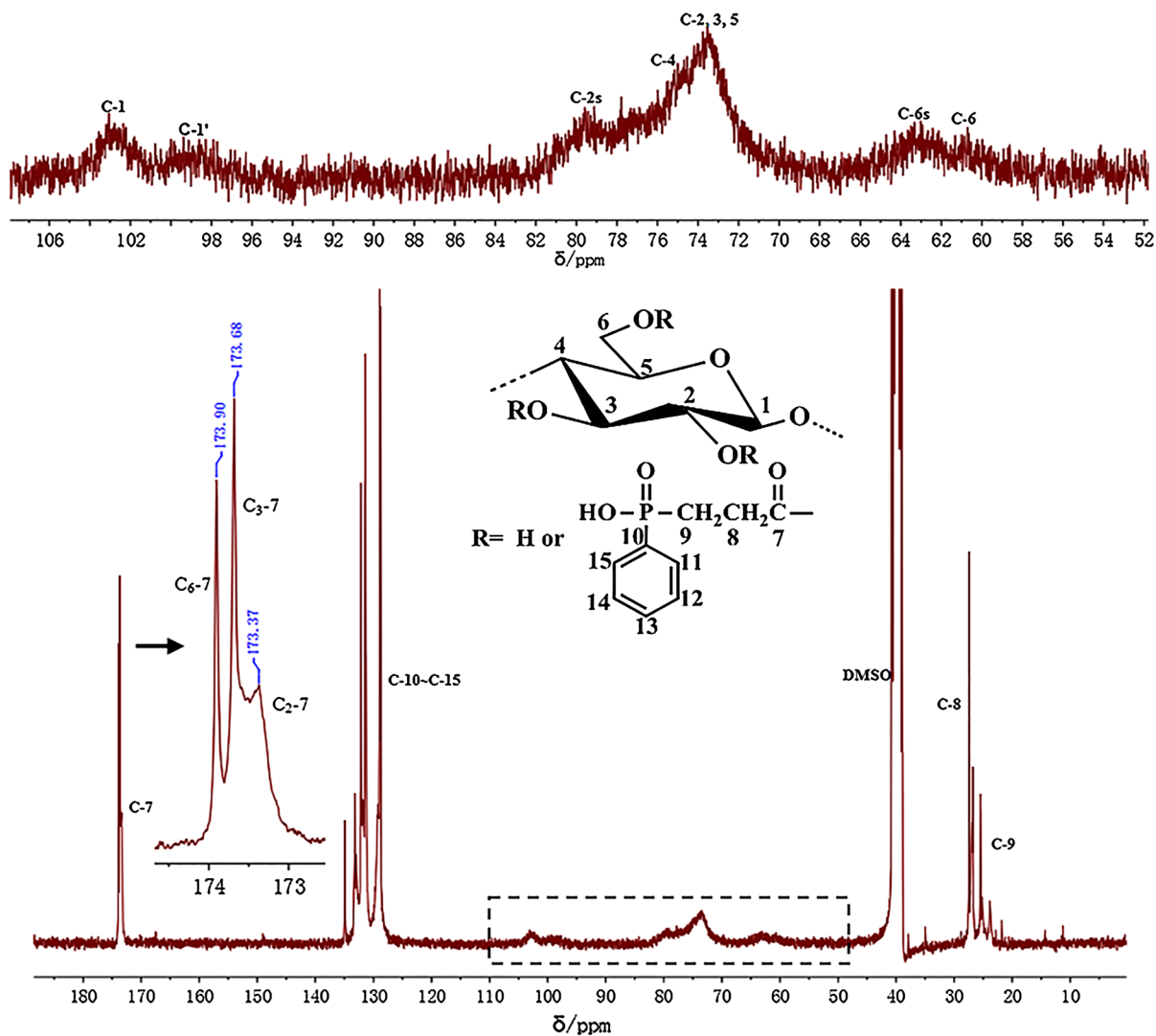
Fig. 2 ^{13}C-NMR spectra of 3#FRC (DS = 0.96)

water), 1,432 cm^{-1} (in plane bending vibration of C–H), and 1,056 cm^{-1} (C–O–C pyranose ring skeletal vibration; Alongi et al. 2014a). Since only the release of physically adsorbed water occurs, relative intensity of all the characteristic peaks almost does not change around 100 °C except for the peak at 1,650 cm^{-1}. With further increase of temperature, relative intensity of the characteristic peaks at 3,400, 2,900, 1,650, 1,432 and 1,056 cm^{-1} all decreases gradually and finally disappears at 350 °C, implying that cellulose is decomposed through dehydration reactions in this

stage. The results are consistent with the TGA results. Meanwhile, two new peaks can be observed clearly above 250 °C. The peaks at 1,730,1,443 and 1,624 cm^{-1} are assigned to C=O and C=C stretching vibration, which further suggests that dehydration reactions of cellulose are carrying out and producing aldehydes, ketones and other olefin compounds. But when temperature reaches 400 °C, these peaks are almost disappeared, which means that a decarboxylation reaction are carrying out and producing combustible gases such as aldehydes, ketones, etc. When

Table 2 Vertical flammability and LOI test for different FRCs and cellulose

NO.	Vertical flammability				LOI	
	Afterflame time (sec)	Afterglow time (sec)	Char length (cm)	Rate of flame spread (mm/s)	Average of LOI (vol %)	[a]Average of LOI (vol %)
Cellulose	30	6	30	7.1	18.6	18.6
2#FRC	0	0	2.5	2.1	27.1	26.2
3#FRC	0	0	1.8	1.5	32.0	30.3
5#FRC	0	0	0.7	0.58	38.7	36.0

[a] 17 %FRC + 3 %CA

the temperature reaches 500 °C, the only obvious peak is the absorption at 1,452 cm^{-1} (condensed aromatics), implying that cellulose decomposes completely and forms relatively stable char layer.
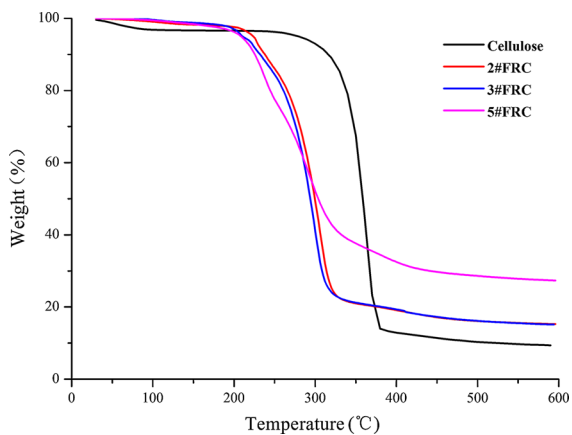
Fig. 3 TGA curves of cellulose and the FRCs

Figure 5 shows the thermal degradation process of FRC (3#FRC). Absorption at 3,400 cm^{-1} (OH) vanishes suddenly at 280 °C, which disappears at lower temperature than in cellulose. This phenomenon can be attributed to the effect of catalyzed dehydration by phosphorus acid. With increasing temperature to 280 °C, the peaks at 1,058 cm^{-1} ascribed to P–O–C group gradually vanish, implying the break of P–O–C structure. The peaks at 1,731 and 1,408 cm^{-1}, assigned to the vibration of C=O group, start to decrease from about 200 °C and almost disappear around 450 °C.

The peak around 1,215 cm^{-1} may correspond to stretching vibration of P=O. When temperature goes up to 300 °C, some new peaks appear. The absorption at 1,584 cm^{-1} attributed to C=C stretching vibration of aromatic structure, keeps its relative intensity all the time, implying that the treated cellulose has not been decomposed completely at 500 °C (Yuan et al. 2012a). On the other hand, the peak at 1,270 cm^{-1}

Fig. 4 FTIR spectra of cellulose during the thermal degradation in the range of RT-500 °C
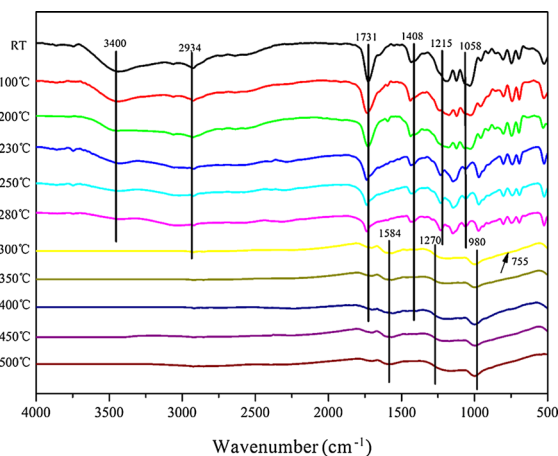
Fig. 5 FTIR spectra of 3#FRC during the thermal degradation in the range of RT-500 °C
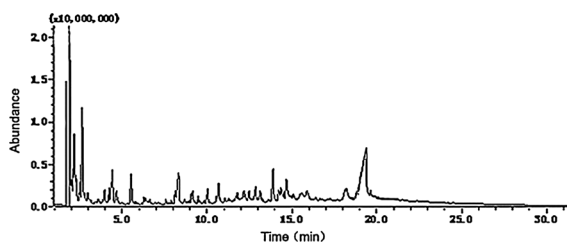
Fig. 6 Py–GC/MS spectrum of cellulose
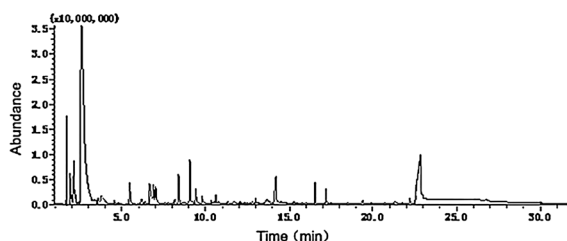
Fig. 7 Py–GC/MS spectrum of 3#FRC

indicates that the phosphate group deviates from the aliphatic structure and then forms poly(phosphoric acid) (PPA) or relinks to aromatic structure. The small peak at 980 cm^{-1} can be ascribed to stretching vibration of P–O–P (Qian et al. 2011). Appearance of the new peak at 755 cm^{-1} implies aromatic structures are formed (Qian et al. 2011; Zhu and Shi 2003).

Py–GC/MS analysis

To investigate formation of the main components of the products in cellulose and 3#FRC pyrolysis process, Py–GC/MS analysis on cellulose and 3#FRC was conducted. Figures 6 and 7 are the Py–GC/MS spectra of cellulose and 3#FRC. Compared with cellulose, number of the peaks in the 3#FRC decreases dramatically, which means that gas products also decrease in thermal degradation (Zhu et al. 2004). As is well known, the pyrolysis vapors of cellulose consist of alcohol/phenol, aldehyde, ketone, furan, benzene ring, ester, ether and other unknown substances (Masuko et al. 2002), and. these gases are usually combustible. It can be observed from Table 3 that the amount of combustible gases pyrolyzed from the 3#FRC is much less than that from cellulose, and the main pyrolysis products of cellulose and 3#FRC were identified in Table 4 and 5. Moreover, more water and carbon dioxide are produced in the 3#FRC pyrolysis process. Water and carbon dioxide have rather important role in antiflaming materials because of their incombustibility, so that it can be concluded that reduction of flammable gases and increase of non-flammable gases can improve flame retardancy of cellulose in thermal decomposition.

Morphology of the Residual Char

The morphologies of chars from the sample at the end of LOI test were investigated by SEM. Figure 8 shows

Table 3 Types and percentages of pyrolyzed products from both cellulose and 3#FRC

Product of pyrolysis	Cellulose		3#FRC	
	Number of peaks	Percent of total area	Number of peaks	Percent of total area
H_2O and CO_2 (CO)	2	48.03	2	58.09
Alcohols	5	16.55	1	
Aldehydes	2	1.34	–	
Ketones	13	8.99	7	3.15
Furans	11	5.77	12	13.06
Benzene	1		–	
Esters	2	0.61	1	4.67
Ethers	5	4.83	3	4.19
Nuceoglucosan	1		1	
P compounds	–		1	1.26
Other substances		5.44		12.07
Unknown		7.09		3.51

Table 4 The main pyrolysis products of cellulose
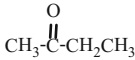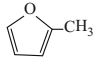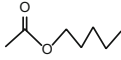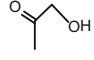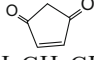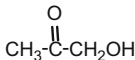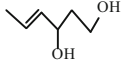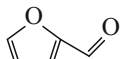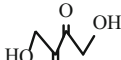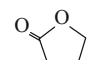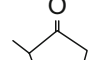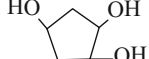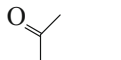
Retention time (min)	m/z	Assigned structure
1.724	18	H_2O
1.894	44	CO_2
1.910	72	$CH_3\text{-}\overset{O}{\overset{\|}{C}}\text{-}CH_2CH_3$
2.1	82	(2-methylfuran structure) $-CH_3$
2.17	130	(ester structure)
2.51	70	(structure)
2.66	74	(hydroxy ketone structure)
2.85	96	(cyclopentenedione structure)
2.98	86	$CH_3CH_2CH_2CH_2CHO$
3.95	74	$CH_3\text{-}\overset{O}{\overset{\|}{C}}\text{-}CH_2OH$
4.23	116	(structure) OH
4.43	76	$CH_3CH_2\text{-}O\text{-}CH_2OH$
5.53	96	(furfural structure)
5.805	144	HO (structure)
7.58	114	HO (structure) OH
7.95	84	(furanone structure)
8.12	84	$CH_3CH_2\text{-}\overset{O}{\overset{\|}{C}}\text{-}CH\text{=}CH_2$
8.33	98	(methylcyclopentanone structure)
8.75	118	HO (structure) OH, OH
8.85	112	O (structure)
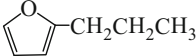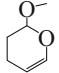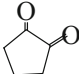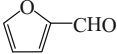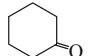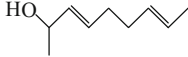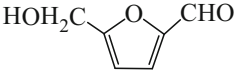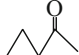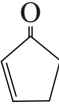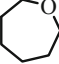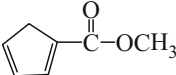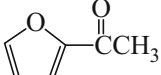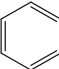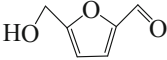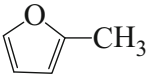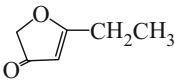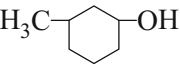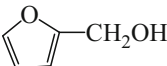
Table 4 continued

Retention time (min)	m/z	Assigned structure
9.095	98	
9.475	110	
10.04	114	
10.68	98	
11.065	68	
11.205	96	
11.295	98	
11.71	140	
11.805	126	
12.015	86	CH$_2$=CHCH$_2$CH$_2$CH$_2$OH
12.195	86	
12.485	82	
13.14	100	
13.9	126	
14.23	98	
14.37	78	

Table 4 continued

Retention time (min)	m/z	Assigned structure
14.525	126	
14.69	126	
15.89	82	
18.185	112	
20.1	114	
20.85	98	

the morphologies of the char residues. From Fig. 8a, many flaws can be seen clearly on the surface of the char residue of cellulose, and this structure is conducive to gas diffusion and heat transfer, which makes the sample burn easily. By contrast, the char layers of the FRCs are dense and compact (Fig. 8b, c, d). Thus, the compact char can serve as a much better physical barrier, which can not only prevent the penetration of oxygen and the combustible gases, but also resist mass and heat transfer. As a result, the underlying polymeric substrate can be protected from attacking by heat flux in a flame.

Morphology and mechanical characterization of FRC fibers

Spinning property of the FRCs will be deteriorated due to the bulky moieties, whereas adding 3 wt% cellulose acetate can improve the spinnability of the solution. As shown in Fig. 9, FRC fibers show a smooth surface and rounded cross section, and the breaking strength of the nascent FRC fibers can reach about 1.2cN/dtex.

High breaking elongation can make a contribution to stretching and orientation, thus further increasing breaking strength of the fibers (Table 6). Moreover, it can be found from Table 2 that the LOI values of the blend fibers with 3 wt% cellulose acetate are still high (26.2 for 2# FRC fiber, 30.3 for 3# FRC fiber, and 36.0 for 5# FRC fiber).

Conclusions

In the present work, homogeneous esterification reactions of cellulose were carried out via in situ activation with Tos-Cl in DMAc/LiCl. The results of FT-IR, 13C-NMR and ICP analysis showed that 3-HPP was grafted onto the backbone of cellulose, and that the highest DS could reach 1.42 when the mole ratio of AGU/3-HPP/Tos-Cl was 1:5:5. After reacting with 3-HPP, flame retardancy of cellulose ester was increased. Meanwhile, the LOI values of cellulose esters were improved gradually with increasing DS, and the highest LOI value could

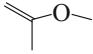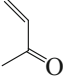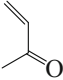**Table 5** The main pyrolysis products of 3#FRC
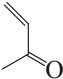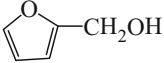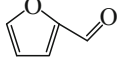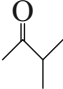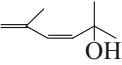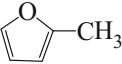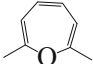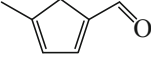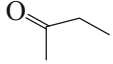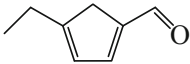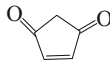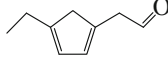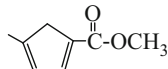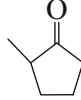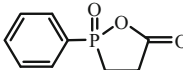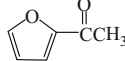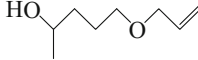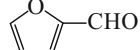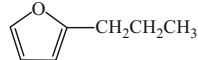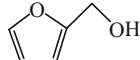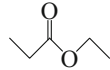
Retention time (min)	m/z	Assigned structure
1.885	18	H_2O
1.97	68	
2.055	72	
2.115	70	
2.15	70	
2.18	70	
2.265	98	
2.605	44	CO_2
5.48	96	
6.68	87	
6.91	126	
7.035	82	
8.395	122	
9.08	110	
9.435	74	
9.79	124	

Table 5 continued

Retention time (min)	m/z	Assigned structure
10.62	96	
12.995	138	
13.505	140	
13.7	98	
14.205	196	
16.545	110	
17.195	144	
19.385	96	
21.77	110	
22.19	98	
23.95	102	

reach 38.7. The results of vertical flame test showed that cellulose treated with 3-HPP had less char length, lower flame spread rate and no afterflame or afterglow time. TGA results revealed that thermal stability of cellulose esters was greatly improved. According to the results of FT-IR and Py–GC/MS, the flame retardant 3-HPP reacting with cellulose could accelerate dehydration action and decrease flammable released products. SEM images reflected the compact char of the FRCs had a positive influence on material in pyrolysis process, and the FRC fibers with 3 wt% cellulose acetate prepared by dry-wet spinning technique were confirmed to possess superior flame resistance.

Fig. 8 SEM photographs of char residue of cellulose and the FRCs

Fig. 9 ESEM images of the FRC fibers

Table 6 Mechanical properties of the FRC fibers

No.	2#FRC fiber	3#FRC fiber	5#FRC fiber
Breaking strength (cN/dtex)	1.19	1.21	1.28
Breaking elongation (%)	85.51	83.12	70.75

References

Alongi J et al (2014a) Caseins and hydrophobins as novel green flame retardants for cotton fabrics. Polym Degrad Stab 99:111–117
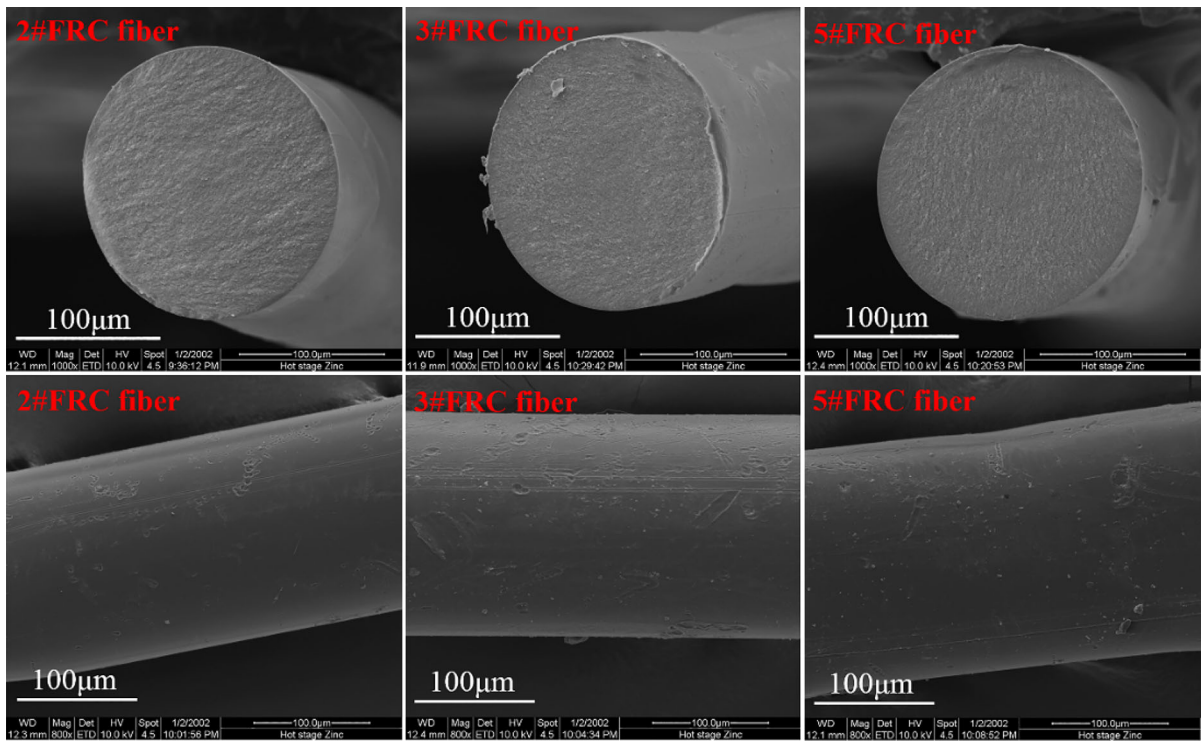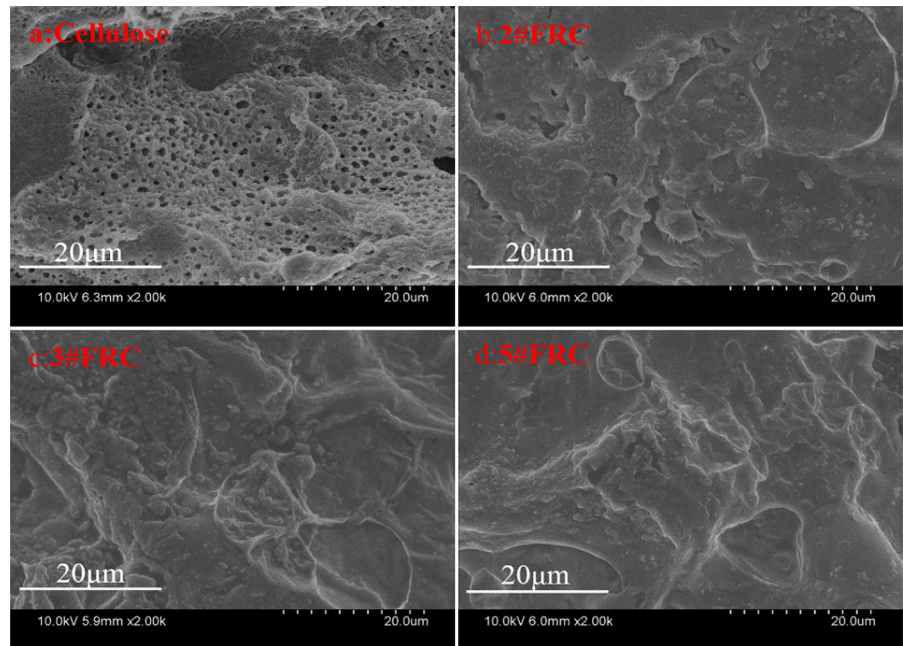
Alongi J, Carosio F, Malucelli G (2014b) Current emerging techniques to impart flame retardancy to fabrics: an overview. Polym Degrad Stab 106:138–149

Bell KD, Graveson I, Ollerenshaw TJ (1997) Fiber production process. U.S. Patent No. 5,690,874

Cao Y, Li H, Zhang J (2011) Homogeneous synthesis and characterization of cellulose acetate butyrate (CAB) in 1-allyl-3-methylimidazolium chloride (AmimCl) ionic liquid. Ind Eng Chem Res 50:7808–7814

Chang S, Slopek RP, Condon B, Grunlan JC (2014) Surface coating for flame-retardant behavior of cotton fabric using a continuous layer-by-layer process. Ind Eng Chem Res 53:3805–3812

Gräbner D, Liebert T, Heinze T (2002) Synthesis of novel ad-amantoyl cellulose using differently activated carboxylic acid derivatives. Cellulose 9:193–201

Hasani MM, Westman G (2007) New coupling reagents for homogeneous esterification of cellulose. Cellulose 14:347–356

Liebert T Cellulose solvents-remarkable history, bright future. In: ACS symposium series, 2010. Oxford University Press, pp 3-54

Hong KH, Liu N, Sun G (2009) UV-induced graft polymerization of acrylamide on cellulose by using immobilized benzophenone as a photo-initiator. Eur Polym J 45:2443–2449

Horrocks AR (2011) Flame retardant challenges for textiles and fibres: new chemistry versus innovatory solutions. Polym Degrad Stab 96:377–392

Horrocks A, Kandola B, Davies P, Zhang S, Padbury S (2005) Developments in flame retardant textiles—a review. Polym Degrad Stab 88:3–12

Huang G, Liang H, Wang X, Gao J (2012) Poly (acrylic acid)/clay thin films assembled by layer-by-layer deposition for improving the flame retardancy properties of cotton. Ind Eng Chem Res 51:12299–12309

Hussain MA, Liebert T, Heinze T (2004) Acylation of cellulose with N, N'-carbonyldiimidazo-activated acids in the Novel solvent dimethyl sulfoxide/tetrabutylammonium fluoride. Macromol Rapid Commun 25:916–920

Köhler S, Heinze T (2007) Efficient synthesis of cellulose furoates in 1-N-butyl-3-methylimidazolium chloride. Cellulose 14:489–495

Lewin M (2010) Handbook of fiber chemistry. CRC Press, Boca Raton

Liang SY, Neisius NM, Gaan S (2013) Recent developments in flame retardant polymeric coatings. Prog Org Coat 76:1642–1665

Liebert TF, Heinze T (2005) Tailored cellulose esters: synthesis and structure determination. Biomacromolecules 6:333–340

Liu W, Chen L, Wang Y-Z (2012) A novel phosphorus-containing flame retardant for the formaldehyde-free treatment of cotton fabrics. Polym Degrad Stab 97:2487–2491

Lu S-Y, Hamerton I (2002) Recent developments in the chemistry of halogen-free flame retardant polymers. Prog Polym Sci 27:1661–1712

Lu F, Cheng B, Song J, Liang Y (2012) Rheological characterization of concentrated cellulose solutions in 1-allyl-3-methylimidazolium chloride. J Appl Polym Sci 124:3419–3425

Lu F, Wang L, Ji X, Cheng B, Song J, Gou X (2014) Flow behavior and linear viscoelasticity of cellulose 1-allyl-3-methylimidazolium formate solutions. Carbohydr Polym 99:132–139

Martin C, Ronda J, Cadiz V (2006) Boron-containing novolac resins as flame retardant materials. Polym Degrad Stabil 91:747–754

Masuko F, Mitani C, Sakamoto M (2002) Pyrolysis and limiting oxygen indices of cotton fabrics. graft copolymerized with oligomeric vinyl phosphonate and/or N-methylolacrylamide. Fire Mater 26:225–234

Muralidhara K, Sreenivasan S (2010) Thermal degradation and burning behaviour of cellulose based and cellulose-silk blended upholstery fabrics. J Sci Ind Res 69:879

Nguyen TM, Chang SC, Condon B, Slopek R, Graves E, Yoshioka-Tarver M (2013) Structural effect of phosphoramidate derivatives on the thermal and flame retardant behaviors of treated cotton cellulose. Ind Eng Chem Res 52:4715–4724

Qian X et al (2011) Combustion and thermal degradation mechanism of a novel intumescent flame retardant for epoxy acrylate containing phosphorus and nitrogen. Ind Eng Chem Res 50:1881–1892

Raus V et al (2012) Activation of cellulose by 1, 4-dioxane for dissolution in N, N-dimethylacetamide/LiCl. Cellulose 19:1893–1906

Reddy PRS, Agathian G, Kumar A (2005) Ionizing radiation graft polymerized and modified flame retardant cotton fabric. Radiat Phys Chem 72:511–516

Rüf H, Kroner G, Dobson P, Männer J, Schrempf C (2010) Flame-retardant lyocell fibers and use thereof in flame barriers. U.S. Patent Application 13/501,684

Rupper P, Gaan S, Salimova V, Heuberger M (2010) Characterization of chars obtained from cellulose treated with phosphoramidate flame retardants. J Anal Appl Pyrolysis 87:93–98

Schnipper A, Smith-hansen L, Thomsen ES (1995) Reduced combustion efficiency of chlorinated compounds, resulting in higher yields of carbon monoxide. Fire Mater 19:61–64

Shafizadeh F, Fu Y (1973) Pyrolysis of cellulose. Carbohydr Res 29:113–122

Shahidi S (2014) Novel method for ultraviolet protection and flame retardancy of cotton fabrics by low-temperature plasma. Cellulose 21:757–768

Shahidi S, Ghoranneviss M (2014) Effect of plasma pretreatment followed by nanoclay loading on flame retardant properties of cotton fabric. J Fusion Energy 33:88–95

Siriviriyanun A, O'Rear EA, Yanumet N (2008) Improvement in the flame retardancy of cotton fabric by admicellar polymerization of 2-acryloyloxyethyl diethyl phosphate using an anionic surfactant. J Appl Polym Sci 109:3859–3866

S-r Wang, Liu Q, Luo Z-y, Wen L, Cen K (2006) Mechanism study of cellulose pyrolysis using thermogravimetric analysis coupled with infrared spectroscopy. J Zhejiang Univ Eng Sci 40:1154

Strlič M, Kolar J (2003) Size exclusion chromatography of cellulose in LiCl/N, N-dimethylacetamide. J Biochem Biophys Methods 56:265–279

Sui X et al (2008) Synthesis of cellulose-graft-poly (N, N-dimethylamino-2-ethyl methacrylate) copolymers via homogeneous ATRP and their aggregates in aqueous media. Biomacromolecules 9:2615–2620

Tsvetkov N et al (2013) Conformational and optical properties of macromolecules of some aliphatic-substituted cellulose esters. Cellulose 20:1057–1071

Wu J, Zhang J, Zhang H, He J, Ren Q, Guo M (2004) Homogeneous acetylation of cellulose in a new ionic liquid. Biomacromolecules 5:266–268

Yang H, Yang CQ (2008) Flame retardant finishing of nylon/cotton blend fabrics using a hydroxy functional organophosphorus oligomer. Ind Eng Chem Res 47:2160–2165

Yoshioka-Tarver M et al (2012) Enhanced flame retardant property of fiber reactive halogen-free organophosphonate. Ind Eng Chem Res 51:11031–11037

Yuan B, Bao C, Guo Y, Song L, Liew KM, Hu Y (2012a) Preparation and characterization of flame-retardant aluminum hypophosphite/poly (vinyl alcohol) composite. Ind Eng Chem Res 51:14065–14075

Yuan H, Xing W, Zhang P, Song L, Hu Y (2012b) Functionalization of cotton with UV-cured flame retardant coatings. Ind Eng Chem Res 51:5394–5401

Zhu S, Shi W (2003) Thermal degradation of a new flame retardant phosphate methacrylate polymer. Polym Degrad Stab 80:217–222

Zhu P, Sui S, Wang B, Sun K, Sun G (2004) A study of pyrolysis and pyrolysis products of flame-retardant cotton fabrics by DSC, TGA, and PY–GC–MS. J Anal Appl Pyrolsis 71:645–655